Silicon carbide polytypes are equilibrium structures

1990 J. Phys.: Condens. Matter 2 5097

(http://iopscience.iop.org/0953-8984/2/23/002)

J. Phys.: Condens. Matter **2** (1990) 5097–5113. Printed in the UK

Silicon carbide polytypes as equilibrium structures

C Cheng, Volker Heine and I L Jones
TCM Group, Cavendish Laboratory, Madingley Road, Cambridge CB3 0HE, UK

Received 15 August 1989

Abstract. The phonon free energy is calculated for several silicon carbide polytypes using a valence overlap shell model. The three most commonly observed polytypes, i.e. ⟨2⟩, ⟨23⟩ and ⟨3⟩, are shown to be thermodynamically stable, with ⟨2⟩ and ⟨3⟩ as the low- and high-temperature phases, respectively, and ⟨23⟩ in between. The long-ranged phonon effect splits the multiphase degeneracy between phases ⟨2⟩ and ⟨3⟩ to which SiC is extremely close at T = 0 K, and it stabilises ⟨23⟩ with a significantly large stability region of 500 K. The calculations of the interatomic displacement–displacement correlations demonstrate how the long-ranged interatomic interactions arise from the phonons. The formation theory of longer-period polytypes is also discussed.

1. Introduction

The purpose of this paper is to study the finite-temperature phonon effects on the stability of SiC polytypes. SiC exists in dozens of different structures called polytypes [1, 2], built up by stacking identical SiC layers in different stacking sequences. The number of layers in a repeat period ranges from one to more than a thousand. The two main interesting questions are why SiC forms polytypes and what physical properties induce such long-ranged interactions.

The present paper is one of a series considering those questions [3–5]. Previous *ab initio* total-energy calculations showed that the majority of SiC polytypes have lower energies than those not observed [3]. In particular, the phases ⟨2⟩ and ⟨3⟩ in the Zhdanov notation [6] (see below) had almost equal energies, the lowest among those calculated. This explains in broadest outline why SiC forms polytypes, almost all of which consist of 2-bands and 3-bands (see below), i.e. of the structures ⟨2⟩ and ⟨3⟩ and their intermediate phases.

Two specific remaining questions are: (i) Are any of these more complex polytypes genuine equilibrium phases, and, if so, which ones? (ii) Also, if so, what phase transitions can one expect between them as a function of temperature T? Such effects require quite long-ranged interactions, and we shall show (section 3) that phonons can indeed produce them. We shall present the results of phonon free-energy calculations relevant to both questions (i) and (ii). These are based on a valence overlap shell model (VOSM) of the interatomic forces, which has been reported and tested previously [7]. The technical details of the phonon calculations are contained in section 2. In particular, we find (section 4) that the phonons produce a phase transition from the phase ⟨2⟩, which we consider is probably the ground state at $T = 0$, to the phase ⟨3⟩ at high temperature. We

0953-8984/90/235097 + 17 $03.50

also investigate the simplest intermediate phase ⟨23⟩ in detail, finding (section 4) that the phonons give it a stability region of several hundred degrees between phases ⟨2⟩ and ⟨3⟩. The exact location of these transitions on the temperature axis is hindered by the accuracy of the *ab initio* total-energy calculations [3, 4], but it seems clear that the phonon free energy makes ⟨23⟩ stable relative to phases ⟨2⟩ and ⟨3⟩. Even higher-order polytypes are considered in section 5. Incidentally the phonons tend to favour the cubic phase ⟨∞⟩, but would suffice to make it stable only at much higher hypothetical temperatures of about 15 000 K. The main results of our calculations were summarised in a brief letter [4].

It will help to outline here the main conceptual framework for our considerations. The structures of SiC polytypes can be considered in terms of 'spins', as there are only two ways of stacking one SiC double atomic layer on top of another, designated as 'up' and 'down' spins. The structure of a polytype is then described in the Zhdanov notation [6] by the widths of the bands of parallel spins. For example, the cubic zincblende SiC is ⟨∞⟩, the wurtzite structure is ⟨1⟩ and a structure with ↓↓ ↑↑ as the repeat unit is ⟨2⟩. Between bands of up and down spin we have an antiphase boundary in the stacking, to be referred to hereafter simply as a 'boundary'. Most of the observed SiC polytypes contain only 2- and 3-bands, i.e. bands of parallel spins with widths of two and three layers, as already remarked. A convenient zero-order model for their free energies is therefore

$$F(T, x) = F_0(T) + x\mu(T) \qquad \text{with } 1/3 < x < 1/2 \tag{1.1}$$

where x is the concentration of boundaries (i.e. the inverse average band width per layer) whose value lies between 1/3 and 1/2. The $F_0(T)$ and $\mu(T)$ are defined so as to make (1.1) exact for the end-phases ⟨2⟩ and ⟨3⟩. The F_0 and μ contain both the intrinsic electronic structure effects (suffix e) at $T = 0$ as found in previous total-energy calculations [3], as well as the phonon contributions (suffix ph) considered here. Thus we write $\mu(T)$ as

$$\mu(T) = \mu_e + \mu_{ph}(T). \tag{1.2}$$

The μ_e is very nearly zero. From matching our results to what can be inferred from experiment [1] (section 4), we believe μ_e is probably slightly negative and we take

$$\mu_e = -5 \times 10^{-4}\ \text{eV} \tag{1.3}$$

within the calculational uncertainty of 10^{-2} to 10^{-3} eV of the *ab initio* total-energy computations [3]. Here and elsewhere all energies will be expressed in eV per SiC pair of atoms.

The main point about (1.1) is that it describes a multiphase degeneracy (MΦD) at a temperature T_0 where

$$\mu(T_0) = \mu_e + \mu_{ph}(T_0) = 0. \tag{1.4}$$

From (1.1) and (1.3), we have that ⟨2⟩ is the stable phase at $T = 0$; whereas we find that $\mu_{ph}(T)$ is positive, so that $\mu(T)$ sweeps through zero at $T = T_0$ given by (1.4), making ⟨3⟩ stable at $T > T_0$. In the simple model (1.1) we have a MΦD at T_0 where the free energy is indepedent of x, i.e. where all phases consisting only of 2-bands and 3-bands in regular and irregular arrangements are all equal (degenerate) in free energy. The first effect of the phonons that we discuss in section 4 is the sweeping of the system through the MΦD at temperature T_0.

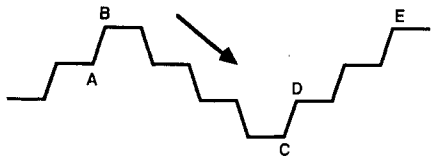

Figure 1. Schematic picture of one chain of atoms in the polytypes with antiphase boundary (see text).

The second effect of the phonons is the splitting of the MΦD by effects beyond those included in (1.1). For the sake of definiteness, we consider in section 4 specifically the simplest intermediate phase ⟨23⟩ with $x = 2/5$. We write

$$F_{\langle 23\rangle}(T) = \begin{cases} [F_0(T) + (2/5)\mu(T)] + \Delta(T) & (1.5a) \\ [(2/5)F_{\langle 2\rangle}(T) + (3/5)F_{\langle 3\rangle}(T)] + \Delta(T) & (1.5b) \end{cases}$$

where the term in square brackets is the zero-order approximation (1.1). Clearly if $\Delta(T_0)$ is negative, then ⟨23⟩ will be a stable intermediate phase between the structures ⟨2⟩ and ⟨3⟩ as T sweeps through the MΦD around T_0. Conversely if $\Delta(T_0)$ were positive, then the MΦD would also be lifted but with a transition directly from ⟨2⟩ to ⟨3⟩. (In this paragraph we are concerned with the lifting of the degeneracy only with respect to the phase ⟨23⟩, ignoring more complicated polytypes.) The $\Delta(T)$ is evaluated (section 4) from computing the three free energies in (1.5*b*) and is found to be negative. Let T_2 and T_3 be the temperatures at which ⟨23⟩ is degenerate with ⟨2⟩ and ⟨3⟩, respectively, when $\Delta(T)$ and $\mu(T)$ are taken into account. We find

$$T_3 - T \simeq -25\Delta(T_0)/(\partial\mu_{\mathrm{ph}}/\partial T)_{T=T_0}. \tag{1.6}$$

The value of (1.6) depends on the choice of μ_e and hence T_0, but with $T_0 = 2400$ K we find a stability range $T_3 - T_2$ of about 500 K! The $-25\Delta(T_0)$ is of order 10^{-4} eV and the surprisingly large range results from the small denominator in (1.6). The latter would of course contribute in a similar way to the possible stability ranges of higher-order polytypes.

It is necessary to invoke a wider conceptual framework to discuss the possible stability of higher-order polytypes. The energy of an arbitrary polytype can be expressed in terms of the interaction between antiphase boundaries. Let I_m be the boundary–boundary interaction (BBI) between boundaries m atomic double layers apart, with superscripts NN and NNN denoting the BBI between nearest- and next-nearest-neighbour boundaries. It is necessary to distinguish I_m^{NN} from I_m^{NNN}, as there are at least two types of boundary, one corresponding to $\uparrow\downarrow$ and the other to $\downarrow\uparrow$ (section 5). The difference is important because the leading terms enter I_m^{NN} and I_m^{NNN} with opposite signs. In terms of BBI, the leading term of $\Delta(T)$ is

$$\Delta(T) \simeq -(1/5)\,(I_4^{\mathrm{NNN}} + I_6^{\mathrm{NNN}} - 2I_5^{\mathrm{NNN}}). \tag{1.7}$$

Various authors [8, 9] have considered the general theory of phase stability in terms of the sign, range and convexity of the I_m. In this context it is necessary to generalise the theory of Bak and Bruinsma [8] to take into account the two types of boundary (section 5). The resulting phase diagram and the conditions to stabilise phases are different from that of Bak and Bruinsma. We have not been able to make a direct comparison of the free energies of higher-order polytypes because of computer limitations. However, we have calculated some further I_m and it is in any case more interesting to consider them from the point of view of trends and the general conditions for polytype stability (section

5). One result is that polytypes with an even number of bands in the Zhdanov symbol seem to be stabilised whereas those with an odd number are not, in agreement with observation. The other is that, in principle, a 'devil's staircase' of an infinite number of intermediate equilibrium phases should not be ruled out, though it requires a rather slow fall-off of the interlayer interactions. Although it is difficult to test, computationally, the slow fall-off of interactions, it can be investigated experimentally. If the condition is satisfied, those at the higher (lower) temperature should have a preponderance of 3-bands (2-bands). It would seem worth while to see if this effect can be observed experimentally.

All our free-energy calculations imply a BBI of moderate range, say four to eight atomic double layers, due to the phonons. Section 3 contains some analysis of this. We may obtain a qualitative picture from figure 1. A longitudinal phonon travelling down the line of bonds B to C will produce a more or less transverse excitation in the row DE beyond the boundary. The discontinuity at the boundary at C will also produce a reflection of the phonon to interact with the discontinuity at the neighbouring boundary at B. The origin of the interaction is therefore a little bit similar to that in the axial next-nearest-neighbour Ising (ANNNI) model [10], where a kink excited on one boundary interacts with another in front of it on the next boundary. However, we believe the actual ANNNI mechanism to be irrelevant to SiC, as argued elsewhere: the energy involved in breaking bonds to form kinks is prohibitive and the nature of ABC stacking would result in a structural fault extending in the form of a line to infinity.

Finally it is necessary to mention some related effects. First, there is the BBI inherent in the electronic total energy of the 'ideal' structure, which we define to have all perfect tetrahedral bond angles and bond lengths equal to that of the cubic phases $\langle\infty\rangle$. This was found to be significant out to I_2 in our previous total-energy calculations, which could not be extended to larger inter-boundary separations [3]. (Note that an interplanar interaction J_n translates into a BBI of I_{n-1}.) However, some estimates of more distant I_m of this origin suggest that it is probably not significant [4, 5], so we will not consider it further here. Secondly, we have the small internal relaxations of the bond angles and bond lengths allowed by the lower symmetry of the polytypes compared with $\langle\infty\rangle$. These have been calculated for the phases $\langle 2\rangle$, $\langle 3\rangle$ and $\langle 23\rangle$, as reported elsewhere [5]. The conclusion there was that such relaxations appear to make a smaller contribution to $\Delta(T)$ than the phonons, though they probably will reduce the stability width of $\langle 23\rangle$ considerably. It was found that the relaxation contribution to Δ is about 2×10^{-6} eV, which will reduce the stability region of $\langle 23\rangle$ at $T_0 = 2400$ K from 500 K to 200 K. However, they contribute significantly to I_2 and I_3, which has the effect of renormalising our $F_0(T = 0)$ and μ_e in (1.1) and (1.2): this has already been taken into account in (1.3). Thirdly, there are several plausible mechanisms to explain polytype formation as non-equilibrium growth structures [11]. We have here considered only the question of whether they can be genuinely stable thermodynamic phases, and found that the $\langle 23\rangle$ can be and probably some higher polytypes similarly. However, we must admit that the free-energy differences beyond $\langle 23\rangle$ become exceedingly small, of order 10^{-7} eV per SiC pair, and we believe that the polytypes with longest repeat distance must involve growth conditions. Nevertheless, what particular structures are likely to result may still be influenced strongly by what is more and less nearly stable as found in the present work.

2. Calculational method

A valence overlap shell model (VOSM) set up previously [7] for cubic SiC ($\langle\infty\rangle$) is used to calculate the phonon frequencies of SiC polytypes in their ideal structures, i.e. structures

Table 1. The phonon free-energy difference of structures ⟨2⟩ and ⟨3⟩ calculated with three different sets of k-points at three different temperatures. The k-point sets are written in the sense of Monkhorst and Pack [13] in the Brillouin zone of ⟨1⟩ and exactly the same sets were used for the two structures.

	$F_{(2)ph}(T) - F_{(3)ph}(T)$ (10^{-5} eV per SiC pair)		
k-point sets	500 K	1500 K	2500 K
(19, 19, 12)	1.44	5.66	9.6
(29, 29, 18)	1.43	5.63	9.6
(49, 49, 30)	1.43	5.62	9.6

with ideal tetrahedral bonding and the same bond length as that of the ⟨∞⟩ structure. In reality, polytypes have slightly different lattice constants and spacings between layers, but it is assumed that the consequent differences in force constants are negligible, so that differences in phonon free energies between polytypes are mainly due to the differences in geometrical structure.

In the model, an atom is described by a charged ion and a massless charged spherical shell bound together by a spring. The short-ranged interatomic interactions include bond stretchings, bond bendings (i.e. bond-angle changes) and the coupling of these two. The total of ten parameters is fitted not only to the available experimental data of phonon frequencies, but also to some frequencies and especially to some eigenvectors calculated from *ab initio* frozen phonon calculations. The latter is crucial for our investigations of the displacement–displacement correlations between atoms, because different phonon models give quite different eigenvectors even when fitted to the same phonon frequencies [12].

The phonon free energy of any structure is described by a set of independent harmonic oscillators, i.e.

$$F_{ph}(T) = \sum_{k,j} \{(1/2)h\omega_j(k) + k_B T \ln[1 + \exp(-h\omega_j(k)/k_B T)]\} \qquad (2.1)$$

where k_B is the Boltzmann constant and $\omega_j(k)$ is the phonon frequency of wavevector k at mode j. The summation is over all modes and over the sampled k-points in the first Brilloun zone of the crystal. Because we require the energy differences between polytypes, exactly the same set of k-points is used for the polytypes ⟨∞⟩, ⟨1⟩, ⟨2⟩, ⟨3⟩ and ⟨23⟩. This is essential for accuracy [3]. We test the convergence of the k-point sampling using three different sets, which correspond to (19, 19, 12), (29, 29, 18) and (49, 49, 30) of the structure ⟨1⟩ in the notation of Monkhorst and Pack [13]. The error in the free-energy differences due to the finite k-point sampling is estimated to be less than 10^{-6} eV per SiC pair (table 1). To investigate the long-ranged phonon interactions, we also calculate the free energies of several long-period SiC polytypes. The k-point sets used in those structures have the same first failure star (a criterion to estimate how good a k-point set is) [13] as that of the set (49, 49, 30), and whenever the energies of two structures are compared, exactly the same k-point set is used for both.

To demonstrate the long-ranged nature of the phonon interactions in SiC, we also calculate the interatomic displacement–displacement correlation tensors and the interatomic force-constant tensors. The equal time correlation tensors depend linearly on

temperature at high temperature. As it is the range of the interactions we look for, we calculate [14].

$$[\langle u(R_1)u(R_2)\rangle/k_B T]_{\text{high temp}} \simeq \frac{1}{N_k(M_1M_2)^{1/2}} \sum_{k,j} \frac{e(R_i|k,j)e^*(R_2|k,j)}{\omega_j^2(k)} \tag{2.2}$$

where $u(R_i)$ and M_i are the displacement and mass of the atom at R_i. Also N_k is the total number of k-points used in the summation. The $\omega_j(k)$ and $e(R_i|k,j)$ are the phonon frequency and displacement pattern (eigenvector) of the atom at R_i for phonon wavevector k of mode j. The structures used in the investigations are $\langle\infty\rangle$, $\langle 1\rangle$, $\langle 2\rangle$, $\langle 3\rangle$ and $\langle 4\rangle$. The k-point set used corresponds to (19, 19, 12) of the structure $\langle 1\rangle$. The convergence of the k-point sampling was found by comparing the results of correlations in the $\langle\infty\rangle$ structure using (19, 19, 8) and (29, 29, 16) meshes: the error is less than 1% of the self-correlations. The interatomic force-constant tensors of polytypes are calculated by Fourier transformation of the dynamic matrix. The k-point set (19, 19, 8) is used and the error due to k-point sampling is less than 0.1% of the self-interaction force-constant tensors.

3. Origin of the long-ranged interactions

The purpose of this section is to present calculations and a theoretical discussion of (i) the moderately long range of the interatomic force constants, which is similar to that of the electronic interlayer interaction and the BBI of relaxations [5] in ideal SiC polytypes, and (ii) the *longer* range of the phonon free-energy interactions in SiC polytypes, as demonstrated by the interatomic displacement–displacement correlations (hereafter 'correlations').

That SiC polytypes exhibit moderately long-ranged interactions has been shown by the previous work [3]. The interlayer interaction energies (J_n) of SiC due to the basic electronic structure in the sense of [3] are significant out to third neighbours. This is really the essential condition for the formation of polytypes. Similarly, the Hellmann–Feynman atomic forces [5] calculated for the ideal structures of $\langle 2\rangle$, $\langle 3\rangle$ and $\langle 23\rangle$ imply that the atomic relaxations in polytypes result in a BBI at least up to I_3, which corresponds to fourth-neighbour interlayer interactions. Both effects are similar in nature to the interatomic force constants in polytypes. The force constant between atoms '1' and '2' is defined as the force that atom '2' feels due to a unit displacement of atom '1' while the atoms in the rest of the system are kept fixed. It can be calculated by a Fourier transform of the dynamical matrix for the phonons [15], which we do for the $\langle\infty\rangle$, $\langle 1\rangle$, $\langle 2\rangle$, $\langle 3\rangle$ and $\langle 4\rangle$ SiC polytypes.

The results for the cubic $\langle\infty\rangle$ SiC are shown in table 2 for various neighbours around a Si atom taken as origin. The pattern around a C atom (not shown) is broadly similar. We see, as expected, a range of a few bond lengths. This is not inconsistent with the VOSM for the phonons with only nearest-neighbour interactions appearing explicitly in the model, apart from Coulomb interactions. The point is that there is a knock-on effect of the electronic shells in the VOSM even though the nuclei are kept fixed in the definition of the force constants. The knock-on of the shells transmits the force to an appreciable distance. The force constants are somewhat stronger along a zig-zag chain of bonds (figure 2) parallel to a (1 1 0) direction. This effect was already pointed out by Fleszar and Resta [15] for Ge, where it was much more noticeable. It is presumably due to the special geometry of the chain. Longitudinal displacements can be transmitted easily along it, and the force constants for that are stronger than the bond-bending force

Table 2. Force-constant tensors at various neighbours relative to a Si atom as origin in ⟨∞⟩ SiC. The Si(n) and C(n) are atoms on the (1 1 0) chain as shown in figure 2. The positions of atoms are written in terms of $a/4$, where a is the lattice constant of phase ⟨∞⟩ in a cubic unit cell.

Order of neighbour	Type of atom	Position of atom	Force-constant matrix (10^{-5} dyn cm^{-1})		
0	Si(0)	(000)	1.5853	0.0000	0.0000
			0.0000	1.5833	0.0000
			0.0000	0.0000	1.5833
1	C(0)	(111)	−0.3176	−0.1628	−0.1628
			−0.1628	−0.3176	−0.1628
			−0.1628	−0.1628	−0.3176
2	Si(1)	(220)	−0.0602	−0.0916	0.0174
			−0.0916	−0.0602	0.0174
			−0.0174	−0.0174	0.0342
3	C	(−311)	0.0283	−0.0137	−0.0137
			−0.0097	−0.0210	0.0195
			−0.0097	0.0195	−0.0210
4	Si	(400)	−0.0169	0.0000	0.0000
			0.0000	0.0088	0.0000
			0.0000	0.0088	0.0000
5	C(1)	(331)	0.0090	0.0122	0.0156
			0.0122	0.0090	0.0156
			0.0017	0.0000	0.0017
6	Si	(−422)	−0.0030	0.0045	0.0045
			0.0020	0.0050	−0.0034
			0.0020	−0.0034	0.0050
6	Si	(422)	−0.0030	−0.0020	−0.0020
			−0.0045	0.0050	−0.0034
			−0.0045	−0.0034	0.0050
7	C	(5−1−1)	0.0064	−0.0025	−0.0025
			−0.0025	−0.0044	−0.0025
			−0.0025	−0.0025	−0.0044
7	C	(33−3)	−0.0040	0.0040	−0.0040
			0.0040	−0.0040	−0.0040
			−0.0040	−0.0040	−0.0040
8	Si(2)	(440)	−0.0044	−0.0081	0.0026
			−0.0081	−0.0044	0.0026
			−0.0027	−0.0027	0.0038
9	C	(53−1)	0.0041	0.0031	0.0006
			0.0039	−0.0022	−0.0022
			−0.0007	−0.0018	−0.0041
10	Si	(620)	−0.0040	−0.0018	0.0004
			−0.0018	−0.0019	−0.0001
			−0.0004	−0.0001	−0.0025

Table 2. *continued*

Order of neighbour	Type of atom	Position of atom	Force-constant matrix (10^{-5} dyn cm^{-1})		
11	C	(533)	0.0028	0.0037	0.0037
			0.0026	0.0007	0.0016
			0.0026	0.0016	0.0007
12	Si	(−4−4−4)	0.0002	−0.0021	−0.0021
			−0.0021	0.0002	−0.0021
			−0.0021	−0.0021	0.0002
12	Si	(444)	0.0002	−0.0021	−0.0021
			−0.0021	0.0002	−0.0021
			−0.0021	−0.0021	0.0002
13	C(2)	(551)	0.0016	0.0030	0.0021
			0.0030	0.0016	0.0021
			0.0006	0.0006	−0.0010
13	C	(−711)	0.0029	−0.0003	−0.0003
			−0.0005	−0.0019	0.0011
			−0.0005	0.0011	−0.0019

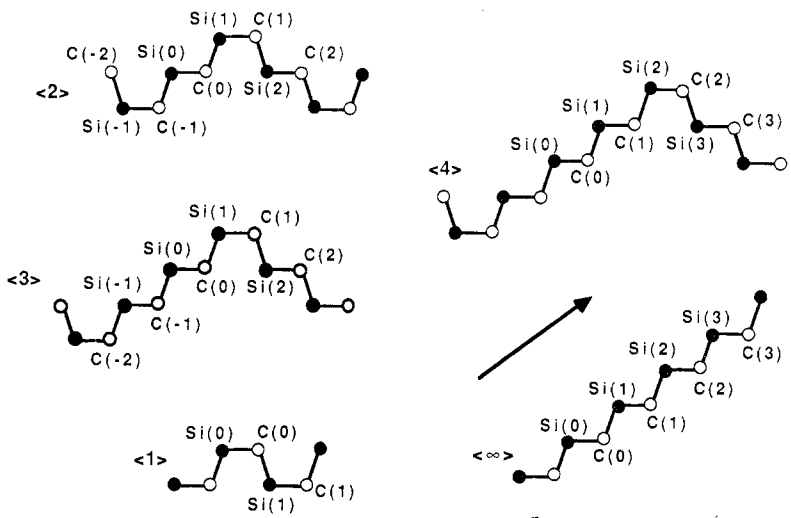

Figure 2. Positions of atoms defined in the five structures ⟨∞⟩, ⟨1⟩, ⟨2⟩, ⟨3⟩ and ⟨4⟩. The full circles represent Si atoms and the open circles C atoms. The arrow gives the direction of the displacement of atom Si(0) and the component taken of the force or displacement at the other atoms.

constants needed to 'go round a corner'. It was already pointed out in connection with figure 1 that going round a corner involved a longitudinal displacement becoming a softer transverse one in the context of polytypes: the same effect applies in the ⟨∞⟩ structure for propagation to atoms other than those in the (1 1 0) chains. The much more isotropic force constants in SiC might be due to the different shell charges of Si and C

Table 3. Responses in the sense of the interatomic force constant in response to a unit displacement of the Si(0) atom in the structures ⟨∞⟩, ⟨1⟩, ⟨2⟩, ⟨3⟩ and ⟨4⟩. The positions of the atoms are illustrated in figure 2. The displacement of Si(0) and the component of the resulting force on other atoms are both taken parallel to the chain direction, as shown in figure 2. All the responses are normalised to the self-interaction, i.e. the restoring force at Si(0).

Atoms	⟨∞⟩	⟨1⟩	⟨2⟩	⟨3⟩	⟨4⟩
Si(0)	1	1	1	1	1
C(0)	−0.3030	−0.3027	−0.3031	−0.3039	−0.3030
Si(1)	−0.0958	0.0110	−0.0975	−0.0958	−0.0957
C(1)	−0.0134	0.0054	0.0145	0.0141	0.0137
Si(2)	−0.0079		0.0018	0.0020	−0.0079
C(2)	0.0029		0.0032	0.0030	0.0030
Si(3)	−0.0017				−0.0023
C(3)	0.0010				0.0015

atoms, i.e. Coulomb effects. The force constants in SiC are therefore moderately long-ranged in all directions, while those in Ge are only strong for the atoms in the (1 1 0) direction.

Although we have shown the moderately long-ranged nature of the force constants in ⟨∞⟩ SiC, the corresponding long-ranged interlayer interactions and the phonon BBI actually result from the changes in the force constants due to the presence of boundaries. As we already know that the interactions are long-ranged, instead of inspecting the general 3 × 3 tensors we look at the response in a direction (chosen to be in the (1 1 0) direction) along a chain to a unit displacement on atom Si(0) also parallel to a chain. The effect of a boundary at various distances from the Si atom are shown in table 3 for the atoms shown in figure 2. Instead of working with a single boundary, which is computationally difficult, the results are taken from calculations on polytypes ⟨1⟩, ⟨2⟩, ⟨3⟩ and ⟨4⟩, so that they include minor contributions from more distant boundaries. All the responses are normalised to the self-interaction in each structure. As the absolute values of these self-interactions in different structures differ from each other by less than 1%, they are all taken to be unity. In table 3 we see the differences caused by a nearby boundary by comparing corresponding atoms (figure 2) in different structures. The effects are significant, but not very large. For example, the force at Si(2) in ⟨∞⟩ and ⟨4⟩ differs from that in ⟨2⟩ and ⟨3⟩, where there is a boundary in between. The difference are of order 1% of the self-interaction. The difference at Si(2) between ⟨2⟩ and ⟨3⟩ is very small due to the effect of a more distant boundary at C(−1) and C(−2), respectively (figure 2). We conclude that the boundary effects of the 'static' interactions (force constants) are significant up to third-neighbour double layer and so are their differences between polytypes, i.e. I_2, but cannot extend much beyond that.

To sum up the above discussion, the force constants and their differences between polytypes show a moderately long range out to third-neighbour atomic double layer in appropriate directions. This range is somewhat surprising in a saturated covalent material, and we believe is analogous to the Friedel oscillations in a metal, though here damped from the existence of the energy gap [16]. The range found in the force constants is the same as seen in the intrinsic interplanar interactions J_n [3] in the sense of [3] and

Table 4. Correlation function between atom Si(0) and the other atom specified in figure 2, for displacements in the same direction as in table 3 and figure 2.

Atoms	⟨∞⟩	⟨1⟩	⟨2⟩	⟨3⟩	⟨4⟩
Si(0)	1	1	1	1	1
C(0)	0.604	0.604	0.604	0.607	0.603
Si(1)	0.396	0.243	0.385	0.387	0.395
C(1)	0.270	0.197	0.255	0.257	0.269
Si(2)	0.200		0.159	0.161	0.196
C(2)	0.150		0.137	0.138	0.144
Si(3)	0.120				0.120
C(3)	0.096				0.101

in the BBI due to atomic relaxation around antiphase boundaries [5]. Indeed, all three effects display the response of the intrinsic electronic structure to a perturbation.

We turn now to the BBI due to phonon free energy. The main point of the present section is that the phonon BBI has a considerably longer range even than that discussed above. It involves how much the atomic vibrations at B in figure 1 'feel' the effect of the boundary at C on the vibrations there. This effect is described by the displacement–displacement correlation function (2.2). It is the displacement of an atom '2' due to the displacement of an atom '1' while all the other atoms in the system are allowed to relax. As the correlation involves a knock-on effect between *atoms* (not just the electron shells), it is expected to be appreciably longer-ranged than the interatomic force constants. This can be seen by comparing correlation response of atoms in the ⟨∞⟩ structure in table 4 to the force constants in table 3. The correlations between atoms decay to one-tenth of the self-correlations at the six-neighbour atom while the force constants decay to one-tenth at the third-neighbour atom. Incidentally, by dividing the phonon bands into various ranges of frequency, we have found that the long-ranged effects are mostly due to the low-frequency end of the acoustic branches. The difference between polytypes is therefore connected with the region where the purely acoustic $\omega(k)$ turns into the flat TA mode so characteristic of the diamond structure and sensitive to stacking arrangement.

The long-ranged BBI correspond to the difference of the long-ranged correlations with and without boundaries. Similar to the above procedure in investigating the 'static' effect of boundaries, the interatomic correlations of ⟨1⟩, ⟨2⟩, ⟨3⟩ and ⟨4⟩ parallel to the chain direction are listed in table 4. The effect of a boundary at the second-neighbour double layers changes the response by up to 4% of the self-correlation, as can be seen by comparing Si(2) and C(2) of ⟨∞⟩ or ⟨4⟩ with ⟨2⟩ or ⟨3⟩. Although the atoms Si(2) and C(2) of ⟨3⟩ are actually closer to Si(0) than those in ⟨∞⟩, the response is still stronger for the latter, where the chain is unbroken. For the third-neighbour layer interaction, the response of Si(3) of ⟨4⟩ is about the same as that of the ⟨∞⟩, because now the factor of distance is balanced by the special long-ranged property of the (1 1 0) chain. The C(3) of ⟨4⟩ is nearer to the origin than the C(3) of ⟨∞⟩ and has a slightly stronger response equal to about 0.5% of the self-correlation, presumably due to the Coulomb interaction. This is an order of magnitude larger than the effect in the 'static' interaction. The 'dynamic' interaction, i.e. the correlation or phonon interactions, thus has range that is much longer than that of the 'static' interactions, i.e. the force constants.

Table 5. Phonon free energies of various polytypes and values of $25\Delta_{ph}(T)$ and $\mu_{ph}(T)$ at six different temperatures. The zero-point phonon energies are also listed and always included at $T > 0$.

Temperature (K)	Phonon free energy (eV per SiC pair)					
	⟨∞⟩	⟨3⟩	⟨23⟩	⟨2⟩	$\mu_{ph}(T)$	$25\Delta_{ph}(T)$
0	0.218 7096	0.218 6817	0.218 6759	0.218 6684	−0.000 0798	−0.0000120
500	0.144 7930	0.144 5077	0.144 5125	0.144 5220	0.000 0858	−0.000 0230
1000	−0.120 3718	−0.120 2998	−0.120 2872	−0.120 2638	0.000 2160	−0.000 0450
1500	−0.509 6324	−0.509 5201	−0.509 5002	−0.509 4639	0.000 3372	−0.000 0645
2000	−0.983 8639	−0.983 7122	−0.983 6853	−0.983 6362	0.000 4566	−0.000 0875
2400	−1.410 425	−1.409 942	−1.409 909	−1.409 850	0.000 552	−0.000 095
3000	−2.112 103	−2.111 873	−2.111 832	−2.111 758	0.000 690	−0.000 125

Another feature one notices is the monotonic decrease of the interactions with distance, for both Si and C atoms. This implies that the sign of the phonon contribution to the interplanar force constants J_n (section 5) would remain the same and its magnitude decrease monotonically. This is important for the stability of higher-order phases, as we shall discuss in section 5.

4. The phase ⟨23⟩

Although this is the shortest section of the paper, it contains the most significant result as has already been summarised in section 1, namely the stability range of ⟨23⟩ as an intermediate phase between ⟨2⟩ and ⟨3⟩. The phonon free energies of ⟨2⟩, ⟨3⟩ and ⟨23⟩, the values of $\mu_{ph}(T)$ (defined in (1.1) and (1.2)) and the values of $25\Delta(T)$ (defined in (1.5)) at various temperatures are listed in table 5. As noted in section 1, equation (1.1) is defined to be exact for the two end-phases, so that $\mu_{ph}(T)$ is given by

$$\mu_{ph}(T) = 6[F_{\langle 2\rangle ph}(T) - F_{\langle 3\rangle ph}(T)]. \tag{4.1}$$

First, we note the positive values of $\mu_{ph}(T)$. It favours phase ⟨3⟩ at high temperature, i.e. the system sweeps through the MΦD (1.4) from phase ⟨2⟩ at low temperature to phase ⟨3⟩ at high temperature.

Secondly, the negative values of $\Delta(T)$ indicate that the MΦD (1.4) is split by phonons and the phase ⟨23⟩ stabilised.

Thirdly, there is the question of the exact value of μ_e and hence of T_0 in (1.2) and (1.4). The experiments suggest that, if ⟨23⟩ is an equilibrium phase as our calculations show, then T_0 must be around 2400 K. According to (1.4) and table 5, this corresponds to the value of μ_e in (1.3). We infer the value of T_0 from the various annealing experiments and observations of growth conditions that have attempted to establish a phase diagram, particularly figure 4 of [17] and tables 5 and 6 of [1]. The stable phases from low temperature to high temperature do seem to be ⟨2⟩, ⟨23⟩ and ⟨3⟩ there, in agreement with our results.

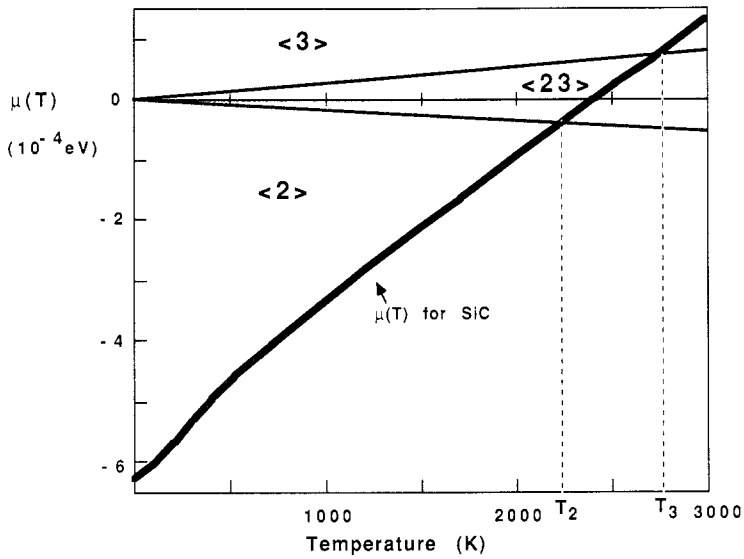

Figure 3. Phase diagram of SiC polytypes. The heavy full curve shows how $\mu(T)$ sweeps through $\mu(T) = 0$ at a temperature $T_0 = 2400$ K. The MΦD of equation (1.4) is split and $\langle 23 \rangle$ is a stable intermediate phase between temperatures T_2 and T_3. The two interphase lines between phase $\langle 23 \rangle$ and phases $\langle 2 \rangle$ and $\langle 3 \rangle$ are two multiphase lines corresponding to phases with dominant 2- and 3-bands, respectively. These phases would split from the two multiphase lines and have finite stability region providing the long-ranged phonon interactions of SiC exist and satisfy certain conditions (section 5).

We now calculate the range of stability for $\langle 23 \rangle$. Expanding the free energies of $\langle 23 \rangle$ (1.5*a*) and $\langle 2 \rangle$ and $\langle 3 \rangle$ (1.1) at temperatures T_2 and T_3 around T_0, one obtains

$$T_0 - T_2 = +10\Delta(T_0)/(\partial \mu_{ph}/\partial T)_{T=T_0} \tag{4.2}$$

$$T_3 - T_0 = -15\Delta(T_0)/(\partial \mu_{ph}/\partial T)_{T=T_0} \tag{4.3}$$

and thus (1.6). The splitting of the MΦD ((4.2) and (4.3)) and the total $\mu(T)$ of SiC as a function of temperature are illustrated in figure 3, which shows clearly the phase transitions due to the effect of temperature on the three free energies.

Finally, we also examine the stability of phase (∞). The status of this phase was left unclear by the experimental data of [17]. The phonon free energies of $\langle \infty \rangle$ at various temperatures are listed in table 5. The phase $\langle \infty \rangle$ has lower phonon free energy than phase $\langle 3 \rangle$ and the difference increases as temperature increases. Therefore, phase $\langle \infty \rangle$ becomes stable at higher temperature than phase $\langle 3 \rangle$. From the phonon free energies at finite temperature and electronic energies [3] at $T = 0$ K of structures $\langle \infty \rangle$ and $\langle 3 \rangle$, we estimate that $\langle \infty \rangle$ would be stable at a hypothetical $T \simeq 15\,000$ K.

5. Higher-order polytypes

In this section we shall discuss the theory of formation for a large number of higher-order polytypes on the basis of BBI due to phonons. We shall start by discussing the theoretical ideas of Bak and Bruinsma [8], who proved the existence of the complete

devil's staircase, i.e. an infinite number of stable commensurate phases, in a one-dimensional model (hereafter referred to as the BB model). They considered 'entities' with interactions I_m between them when the two entities considered are distanced m lattice spacings apart. Three conditions on I_m are required to give an infinite number of phases as the chemical potential β for introducing new entities is varied:

(i) The I_m are repulsive, i.e.

$$I_m > 0. \tag{5.1}$$

(ii) The I_m are convex, i.e.

$$I_{m+1} + I_{m-1} > 2I_m. \tag{5.2}$$

(iii) The I_m have infinitely long range.

A more general theory and criteria for the existence of an infinite number of phases in terms of general interactions, e.g. including not only pairwise interactions, were formulated by Fisher and Szpilka [9]. This general theory, when applied to the model of Bak and Bruinsma, requires the same conditions as the above three to stabilise an infinite number of phases.

As mentioned in the first section, the energies of polytypes can be written in terms of a chemical potential β and interactions I_m between antiphase boundaries. These boundaries can be seen to be similar to the interacting entities in the BB model. However, for SiC, there are at least two kinds of BBI. They correspond to interactions between like boundaries, i.e. between $\downarrow\uparrow$ and $\downarrow\uparrow$ or between $\uparrow\downarrow$ and $\uparrow\downarrow$, and between unlike boundaries, i.e. $\uparrow\downarrow$ and $\downarrow\uparrow$. The two cases differ by having an odd or even number of boundaries in between the two boundaries considered. One can clearly see their difference by writing the energy of polytypes in terms of the pairwise interlayer interaction in the sense of [3], i.e.

$$E = E_0 - \sum_n J_n \sum_i s_i s_{i+n} \tag{5.3}$$

where J_n is the nth-neighbour interlayer interaction energy and $s_i = +1$ or -1 for an up-spin or down-spin SiC layer (section 1). Note that one can express the energy of an arbitrary polytype either in terms of the BBI or in terms of the interlayer interaction model (5.3). In terms of the pair interlayer interaction energy J_n, we have that the energy for introducing a boundary is

$$\beta = 2 \sum_i iJ_i \tag{5.4}$$

and the interaction between boundaries is

$$I_m^{\text{even}} = -4 \sum_{i=m+1} (i - m)J_i = -I_m^{\text{odd}}. \tag{5.5}$$

Note that these two different BBI have opposite sign! As I_m^{even} and I_m^{odd} cannot both be repulsive, it implies changes of the phase diagram from the one in the BB model.

A further complication arises in trying to extend a Bak–Bruinsma analysis to SiC, namely the model (5.3) is a simplification of the energy expression for a general polytype.

Table 6. Contributions to J_n from the phonon free energy.

Temperature (K)	Energy (10^{-4} eV per SiC pair)								
	J_1	J_2	J_3	K_3	J_3'	J_4''	J_5''	J_5^{Δ}	J_6''
500	0.334	0.042	0.008	−0.009	0.020	0.002	0.000	0.012	0.001
1500	1.404	0.128	0.026	−0.026	0.060	0.005	0.001	0.032	0.002
1500	2.398	0.215	0.042	−0.045	0.102	0.008	0.004	0.053	0.003

The general expression contains in addition to (5.3) some terms that are formally multilayer interactions, the first of which is

$$K_3 s_i s_{i+1} s_{i+2} s_{i+3}. \tag{5.6}$$

The analysis of Shaw and Heine [18] has shown that such terms arise from the fact that a given layer, as well as having up or down 'spin', can be laterally in either an A, B or C position relative to another layer in the usual sense of stacking layers in the diamond structure. Thus (5.6) is a modification of the interaction J_3 between layers i and $i+3$ depending on their relative lateral position, which is determined by the spins of the layers $i+1$ and $i+2$ in between. Such terms could introduce wholly new phases into the phase diagram if they were sufficiently large to overwhelm the effect of all other shorter-ranged interactions. For example, if (5.6) were sufficiently large, it would stabilise a phase ⟨31⟩, which does not occur in the model (5.3) with all $J_n = 0$ for $n \geqslant 4$. However, in what follows we shall consider the effects of J_n only, for two reasons. First, the monotonic decrease of correlations between atoms in the different structures of table 4 suggests that it is unlikely that the multilayer interactions are strong enough to stabilise new phases. Secondly, when we consider a particular MΦD, e.g. that between ⟨2⟩ and ⟨3⟩, or that between ⟨2⟩ and ⟨23⟩, etc., the J_n and K_n of the phases on the MΦD are always in a fixed combination for low n. For example, for the MΦD (1.4), the fixed combination for $n = 3$ is $J_3 - (4/3)K_3$, which we shall term J_3'. Thus, within the context of one particular MΦD, the more general model is nearly equivalent to the simpler of (5.3) with modified values of the parameters. The further discussion will therefore be restricted to the simplified model (5.3) with J_n only, except that when quantitative values are involved we shall consider the effective J_n. There are two kinds of effective J_n that we shall mention here. One is J_n', which is of the MΦD considered, and the other is J_n^{Δ}, which corresponds to the leading term to split a MΦD.

We present in table 6 the phonon free-energy contributions to nth-neighbour interlayer interaction for $n = 1$ to 6 at various temperatures. For $n = 1$ to 3, they are in addition to the intrinsic contributions of the electronic structure [3]; for $n \geqslant 4$, the phonon free energy dominates, as already discussed (sections 1 and 3). For J_1 to J_3, the values were obtained by calculating the phonon free energies of ⟨∞⟩, ⟨1⟩, ⟨2⟩, ⟨3⟩ and ⟨23⟩, five phases being needed to get the appropriate combination of J_3 and K_3 in the sense of J_3' just stated. The values of fourth to sixth interlayer interactions were obtained approximately as the leading terms in the phonon free-energy difference between ⟨8142⟩ and ⟨9132⟩, ⟨7152⟩ and ⟨8142⟩, and ⟨9162⟩ and ⟨10 152⟩ respectively. These leading terms (called J_n'') are the sum of J_n ($n = 4$, 5 and 6) and the corresponding K_n (there are two, five and nine K_n for $n = 4$, 5 and 6 respectively). We also listed the values of J_5^{Δ} obtained from $\Delta(T)$. The large difference between J_5 and J_5^{Δ} comes from three sources. The first

one is the uncertainty of calculations, which we estimate to be less than 10^{-6} eV (section 2). The second one is due to the different combinations of J_5 and K_5 (there are five different multilayer interactions that are part of the fifth-neighbour interactions), which we judge to be the major factor. The third source is the longer-ranged interactions J_n and K_n for $n > 5$, which might also have a minor effect. We thus conclude that the values of K_n are about the same order as those of J_n and it is important to take appropriate effective J_n, i.e. J_n', for MΦD and J_n^{Δ} in considering the splitting of the MΦD.

We now discuss whether one can extend the argument of Bak and Bruinsma to prove the existence of a complete devil's staircase with an infinite number of phases in the splitting of our MΦD of ⟨2⟩ and ⟨3⟩ or SiC. The main point is clearly to take into account the essential difference expressed in (5.5) from their model. We start by noting that the J_n in table 6 are all positive and monotonic within the calculation uncertainty. From the correlation calculations (section 3), we may justifiably extrapolate from table 6 to say that we expect the effective J_n from the phonon free energy to be (i) all positive, (ii) decreasing monotonically and (iii) of infinite range in principle. It further seems that we also have the further condition (iv):

$$I_m^{\text{even}} \simeq -I_m^{\text{odd}} < 0 \tag{5.7}$$

which leads to the pair of convex conditions

$$I_{m+1}^{\text{odd(even)}} + I_{m-1}^{\text{odd(even)}} - 2I_m^{\text{odd(even)}} = +4J_m > 0 \; (-4J_m < 0). \tag{5.8}$$

In the BB model, I_m^{odd} and I_m^{even} are identical. However, to stabilise phases with even (odd) number of bands in the Zhdanov symbol (hereafter as even (odd) phases) usually requires the convex condition of an I_m that has an odd number of bands in between the two boundaries considered. The condition (5.8) thus has the important consequence that the leading term of the condition to stabilise odd phases disfavours the stabilisation. To push the analysis one step further, we consider specifically the stability of the phases $\langle (22)^n 23\rangle$ and $\langle (22)^{n-1}223\rangle$ with respect to ⟨2⟩ and $\langle (22)^{n-1}23\rangle$. Both phases are stable in the BB model. It is not difficult to show that, from the leading terms in J_n, to stabilise $\langle (22)^n 23\rangle$ requires

$$J_{m-2} < 2J_m \qquad m = 4n + 5 \tag{5.9}$$

and to stabilise phase $\langle (22)^{n-1}223\rangle$ requires

$$J_{m-2} < J_m. \tag{5.10}$$

The condition (5.10) is not physical, as the interactions would have to increase with distance and diverge at infinity. The even phase $\langle (22)^n 23\rangle$ is thus more favourable than the odd phase $\langle (22)^{n-1}223\rangle$. Similarly, the stability condition for the even phase $\langle 23(33)^n\rangle$ is

$$J_{m-3} < 2J_m \qquad m = 6n + 5 \tag{5.11}$$

while the condition for the odd phase $\langle 233(33)^{n-1}\rangle$ suffers from the same divergence as (5.10), namely

$$J_{m-3} < J_m.$$

The even phases $\langle (22)^n 23\rangle$ and $\langle 23(33)^n\rangle$ are therefore stable if the additional conditions (5.9) and (5.11) are satisfied. These additional conditions arise from the elimination of the odd phases. They require a rather slow fall-off of the J_n with distance, i.e. at least

slower decay than $J_n = (2)^{-n/2}$ for $\langle(22)^n23\rangle$ and $J_n = (2)^{-n/3}$ for $\langle23(33)^n\rangle$. It is the effective J_n that should be taken here. From the limited calculated data of J_n in table 6, we cannot draw a definite conclusion. However, the slow fall-off of the force constant (table 2) and correlations (table 4) suggest that it cannot be completely ruled out.

Other difficulties arise with the more complex phases, which we shall not discuss in detail. However, condition (5.8) of SiC is an indication in the direction that generally even phases are more favourable. This arises as follows. Let the Zhdanov symbol be M layers long. The term $J_M s_i s_{i+M}$ always enters with positive (negative) sign in the energy (5.3) of the polytype for an even (odd) number of bands. Relative to its neighbours, it has a leading term proportional to

$$2I_M - I_{M+1} - I_{M-1}. \tag{5.12}$$

If the structure has an even number of bands in M layers, then the interactions in (5.8) will be for an odd number of boundaries in between, so from (5.8) the value of (5.12) is negative, thus stabilising the polytype.

A very different approach is from the point of view of the branching process, which was discussed by Duxbury and Selke [19] and de Fontaine [20]. In the case of SiC, phases $\langle2\rangle$ and $\langle3\rangle$ are actually made of the units 22 and 33. We have already deduced the existence of phases $\langle23\rangle$. The intermediate phases between $\langle23\rangle$ and $\langle2\rangle$ can be viewed as pairs of bands 23 being inserted in a background of pairs 22. Thus the pair 23 becomes the 'entity' in the sense of the BB model while $\langle2\rangle$ is the 'empty' background. The phases between $\langle23\rangle$ and $\langle3\rangle$ can be treated similarly. This process will only end up with even phases. Note that this makes quite a difference to the phase diagram. For example, the phase intermediate between $\langle23\rangle$ and $\langle2223\rangle$ is $\langle222323\rangle$, which does not occur in the staircase of the BB model. In the BB model the distance to the pth-neighbour boundary in a structure is either r_p layers or $r_p + 1$ layers. For the new phases, this is no longer true. For example, in phase $\langle222323\rangle$, the possible distances to the third-neighbour boundary are six, seven and eight layers because the 2-bands and 3-bands in the structure are not as evenly distributed as before. Thus the analysis of BB, which relies on this fact (combined with the convexity condition), can no longer be carried through. However, for the pth-neighbour boundary, where p is an even number, this property is still retained. This also comes from taking the basic building blocks as 22, 23 and 33. We therefore consider it likely that there is also an infinite sequence of these phases, though no general proof is possible. While the mapping in terms of pairs of bands into the BB model is formally correct in an abstract sense, unfortunately difficulties appear when trying to adapt the detailed algebra, as we saw in (5.9) and (5.11).

We conclude from the above discussion that, first, all stabilised SiC polytypes are more likely to have even number of bands in the Zhdanov symbol. Secondly, in addition to the convex condition, other conditions are needed actually to stabilise long-period phases because of the elimination of phases with an odd number of bands in a period. They depend on quantitative conditions on the J_n. A devil's staircase of an infinite number of phases might be present; it requires a slow fall-off of interlayer interactions. All the above discussion considers the polytypes as equilibrium phases. The stability range from the higher-order ones becomes rather small, though not as narrow as one might expect because of the smallness of the denominator in (1.6), which always enters the stability range. For example, we already estimated $\Delta T \simeq 500$ K for phase $\langle23\rangle$ in section 4. However, the free-energy differences become tiny, as is clear from table 6, and one might wonder about the ability of the system to distinguish between phases, i.e. what is the time for equilibrium to be established. There are plausible growth

mechanisms for the origin of polytypes [13], as mentioned in section 1, which must be operative for the ones with very long repeat distances. Nevertheless, the broad types of structure that grow must presumably still be influenced by the considerations discussed above, in particular the even number of bands in the Zhdanov symbol.

References

[1] Jepps N W and Page T F 1984 *Prog. Cryst. Growth Charact.* **7** 259

[2] Pandey D and Krishna P 1975 *J. Cryst. Growth* **31** 66; 1982 *Curr. Topics Mater. Sci.* **9** 415; 1983 *J. Cryst. Growth Charact.* **7** 213

[3] Cheng C, Needs R J, Heine V and Churcher N 1987 *Europhys. Lett.* **3** 475; Cheng C, Needs R J and Heine V 1988 *J. Phys. C: Solid State Phys.* **21** 1049

[4] Cheng C, Heine V and Needs R J 1990 *Phys. Rev. Lett.* submitted

[5] Cheng C, Heine V and Needs R J 1990 *J. Phys.: Condens. Matter* **2** 5115

[6] Zhdanov G R 1945 *C.R. Acad. Sci USSR* **48** 43

[7] Cheng C, Kunc K and Heine V 1989 *Phys. Rev.* B **39** 5892

[8] Bak P and Bruinsma R 1982 *Phys. Rev. Lett.* **49** 249

[9] Fisher M E and Szpilka A M 1987 *Phys. Rev.* B **36** 644

[10] Von Boehm J and Bak P 1979 *Phys. Rev. Lett.* **42** 122; Fisher M E and Selke W 1980 *Phys. Rev. Lett.* **44** 1502

Yeomans J 1988 *Solid State Physics* vol 41 (New York: Academic) p 151

[11] Frank F C 1987 *Phil. Mag.* A **56** 263

Pandey D and Sutton A P 1990 to be published

Pirouz P 1989 *Proc. Sixth Int. Symp. on Structure and Properties of Dislocations in Semiconductors* ed S G Roberts and P R Wilshaw (Bristol: Institute of Physics)

[12] Kunc K and Martin R M 1981 *Phys. Rev.* B **24** 2311

[13] Monkhorst H J and Pack J K 1976 *Phys. Rev.* B **13** 5188

[14] Maradudin A A, Montroll E W, Weiss G H and Ipatova I P 1971 *Theory of Lattice Dynamics in the Harmonic Approximation* (New York: Academic) p 62

[15] Fleszar A and Resta R 1986 *Phys. Rev.* B **34** 7140

[16] Sokel R and Harrison W A 1976 *Phys. Rev. Lett.* **36** 61

[17] Knippenberg W F 1963 *Philips Res. Rep.* **18** 161

[18] Shaw J J A and Heine V 1990 *J. Phys.: Condens. Matter* **2** 4351

[19] Duxbury P M and Selke W 1983 *J. Phys. A: Math. Gen.* **16** L741; Selke W and Duxbury P M 1984 *Z. Phys.* B **57** 49

[20] de Fontaine D 1984 *J. Phys. A: Math. Gen.* **17** L713